

Surface micromachined membranes for tunnel transducers

Joyce Wong^{a)} and Axel Scherer

Electrical Engineering and Applied Physics, Caltech, Pasadena, California 91125

Thomas George

Jet Propulsion Laboratory, Pasadena, California 91109

(Received 30 May 1997; accepted 31 July 1997)

We have developed low-temperature surface micromachining procedures for the fabrication of suspended $\text{SiO}_2/\text{Si}_3\text{N}_4$ membranes. This fabrication method was integrated with electron beam lithography, anisotropic ion etching, and electroplating to construct electrostatically deflectable tunnel transducers. We show the structures and some preliminary measurements on the performance of these monolithic devices. © 1997 American Vacuum Society. [S0734-211X(97)09906-X]

I. INTRODUCTION

Surface micromachining of thin-film membranes holds the prospect of fabricating monolithic sensor devices with significantly reduced size, mass, and power consumption.^{1,2} Here, we describe a new procedure for constructing monolithic tunnel transducers by using the combination of sacrificial photoresist, room-temperature sputter deposition, electron beam lithography, and metal electroplating. We have developed this low-temperature surface micromachining technique for the fabrication of ultrathin flexible membrane devices in which the accurate measurement of membrane deflection can be used for the sensitive measurement of vibrations, mass, and magnetic fields. With low-temperature micromachining technology, we expect to be able to integrate such sensors on commercially available very large scale integrated (VLSI) driving circuits. In this article, we describe the methods which we use to miniaturize such flexible membrane detectors by nonconventional microfabrication techniques, and show how we form tunnel transducers.

A successful microfabrication approach should be able to fabricate tunneling structures with low tolerances, low membrane deflection voltages, increased packing density of sensors, and reduced crosstalk in detector arrays. Moreover, microfabrication of micromachined sensor arrays with low operating powers on silicon substrates are expected to enable the development of large numbers of reliable and robust monolithic elements which can be ultimately integrated with complementary metal-oxide-semiconductor-compatible driving circuitry. To fabricate the tunneling tip of our transducers, we use a method similar to the Lithographie, Galvanoformung, Abformung process, which was originally developed for the electroplating of microstructures using polymer molds defined by x-ray lithography. However, our technique relies on electron beam lithography and anisotropic ion etching to form the electroplating mold, which results in high resolution and good alignment accuracy of microstructures.

II. PROCEDURE

Low-temperature surface micromachining tools have been previously developed for the fabrication of digital micromirror devices.³ The surface micromachining technique which we have optimized uses a similar process based on hard-baked photoresist defined by optical lithography as a sacrificial layer. The sacrificial layer is then encapsulated by rf magnetron sputter deposition with a coating of SiO_2 or Si_3N_4 followed by a thin Au contact film. Within this photoresist mold, metal pins can then be fabricated by using electron beam lithography followed by directional oxygen etching and electroplating. Finally, the photoresist is removed by an isotropic oxygen plasma etch, and only the hollow membrane shell, the contact layers, and the electroplated tip remain. This procedure defines a supported flexible plate separated from the silicon substrate by a predetermined distance, i.e., the original photoresist layer thickness. The sputter-deposited dielectric layer serves both as a rigid membrane material as well as an electrical isolation layer. An electrostatic field can be applied between the top and bottom contact metal to deflect the membrane at a desired frequency. The amplitude of deflection can then be determined by measuring the tunneling current between an electroplated tunneling tip and the metal-coated deflecting membrane. Conversely, this device can be operated in feedback mode in which the electrostatic deflection voltage necessary for constant tunneling current can be monitored.

Figure 1 shows a schematic flow diagram describing the fabrication sequence which we have developed to define electrostatic tunnel transducers. We start with conventional photolithography, Au/Cr metallization, and chemical etching to define and electrically isolate all deflection electrodes and electromagnetic sensor electrodes. Then, we deposit a sacrificial hard-baked photoresist layer followed by room-temperature silicon dioxide deposition to define the thin dielectric deflection membrane which is sandwiched between two gold electrode layers. Following this membrane deposition, we use high resolution electron beam lithography followed by reactive ion etching to define a small hole into the gold, through the silicon nitride membrane, through the second gold contact, and through the hard-baked photoresist. After this etch, we use electroplating of nickel to deposit a

^{a)}Electronic mail: joyceyw@cco.caltech.edu

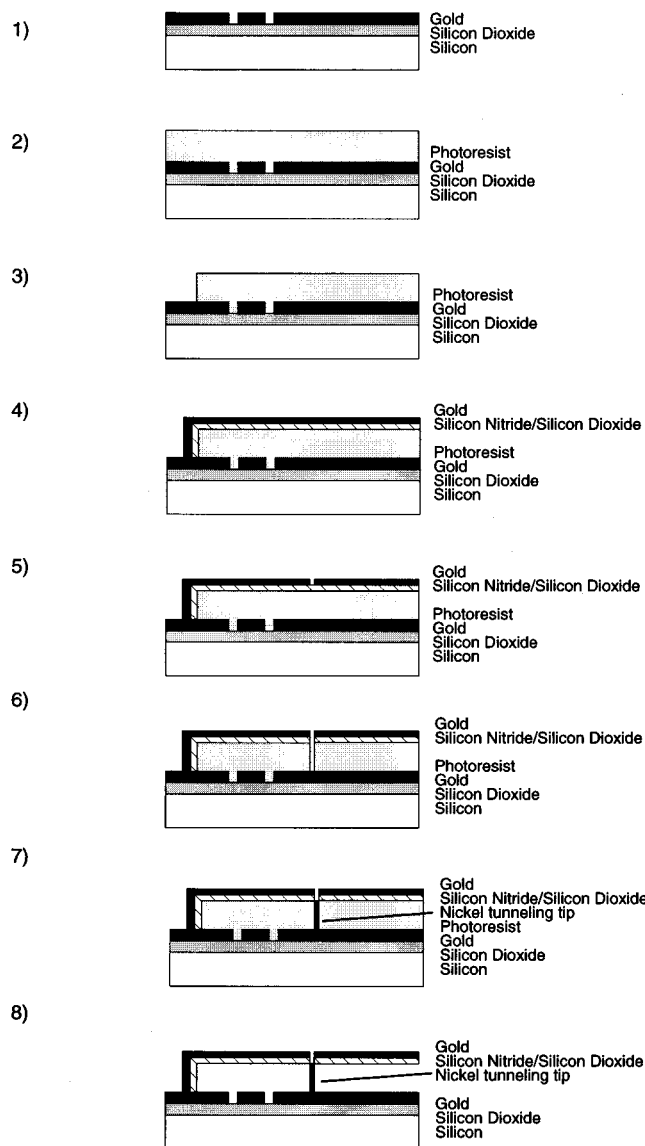
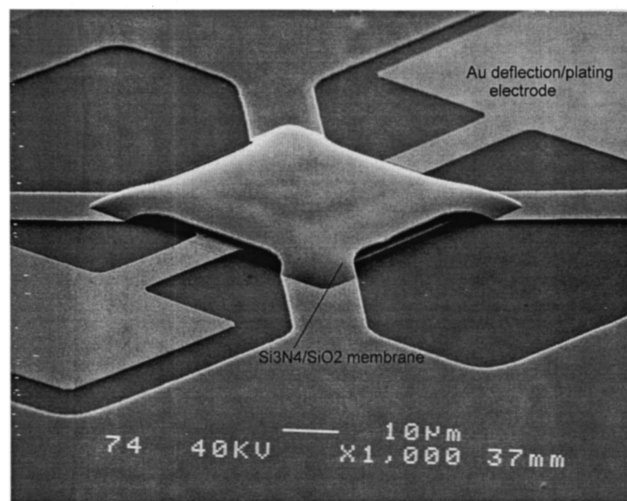


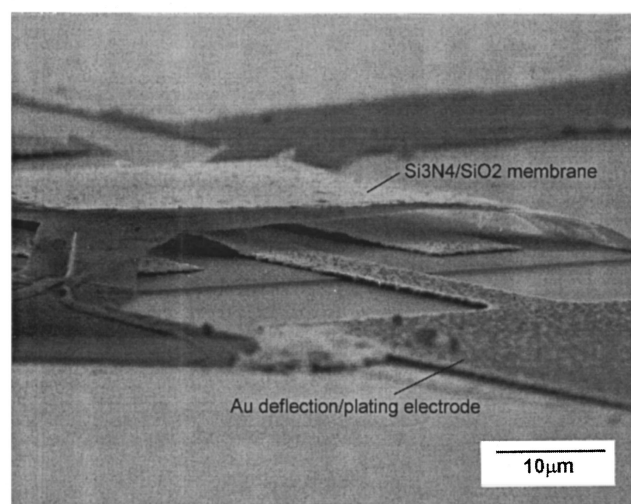
FIG. 1. Schematic diagram of the processing sequence for the fabrication of sensor devices.

small magnet within the 200 nm wide etched hole. If desired, the precise distance between the magnet or tip and the deflection membrane can be monitored during the plating process by using an *in situ* resistance measurement between the membrane and tip contacts. The membrane shape is determined by another optical lithography process followed by a reactive ion etch which also exposes the contacts to the deflection electrode and the tunneling tip. Finally, to complete the micromachined sensor, we use a low-voltage isotropic oxygen plasma etch to remove the sacrificial hard-baked photoresist from underneath the flexible membrane.

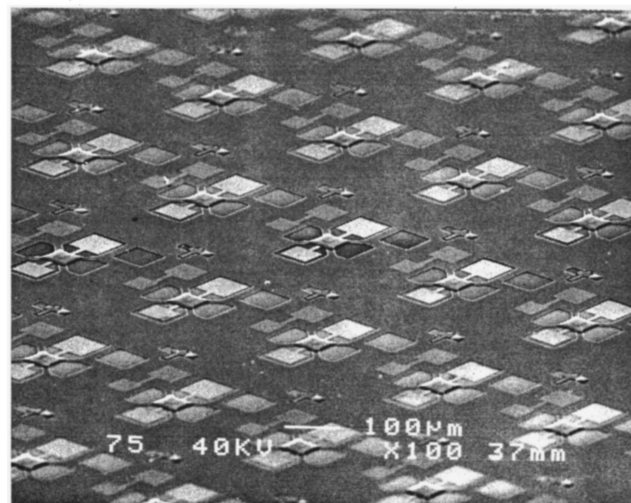
Figure 2(a) shows an electron micrograph of a typical membrane after removal of the photoresist, which shows the deflection and tip electrodes as bright areas underneath the thin SiO_2 film. In this case, the distance between the membrane and the deflection electrodes is approximately $3\ \mu\text{m}$, and the oxide thickness is approximately 100 nm. Figure



(a)

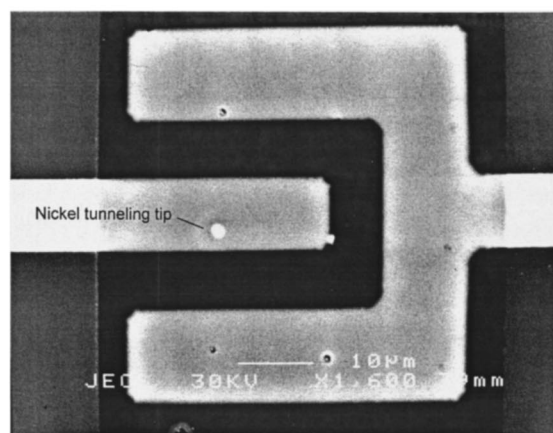


(b)

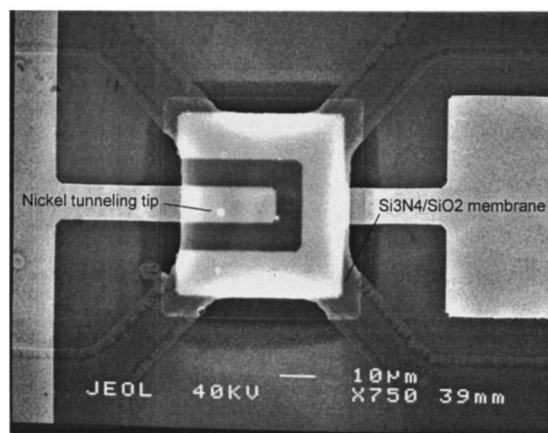


(c)

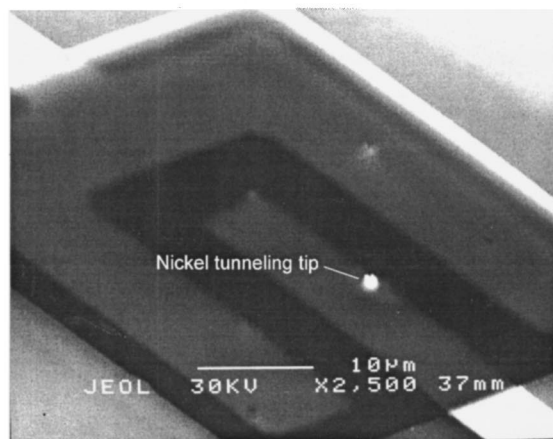
FIG. 2. (a) SEM micrograph of a typical membrane after removal of the sacrificial photoresist. (b) SEM micrograph of a typical membrane (tilted at 70°) after removal of the sacrificial photoresist. (c) SEM micrograph of an array of $50\ \mu\text{m} \times 50\ \mu\text{m}$ sensor devices.



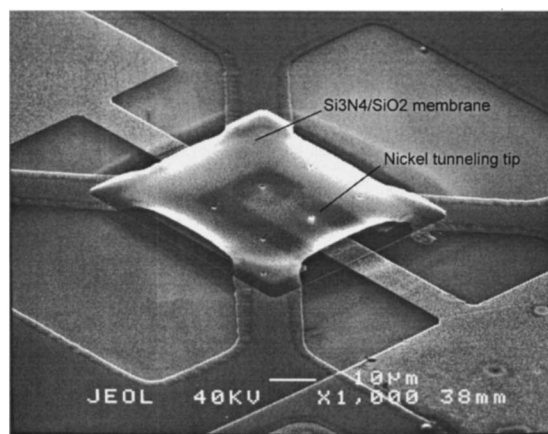
(a)



(c)



(b)



(d)

FIG. 3. (a) Top, (b) angled (tilted at 60°) view of a membrane sample through which an array of holes was etched, followed by nickel plating. (c) Top, (d) angled (tilted at 60°) view of a sensor device with an electroplated nickel tip underneath the membrane.

2(b) shows a scanning electron microscope (SEM) micrograph of the same membrane sample tilted to approximately 70°, which shows that the photoresist layer has been completely removed after a 6–9 h oxygen etch in a SPI-IIA plasma etcher at 45 W. These individually addressable membranes were fabricated in arrays with approximately 350 μm center spacing [Fig. 2(c)]. Fabrication of the tunneling tip underneath the membrane requires three processing steps: First, electron beam lithography is used to expose and develop 200 nm diameter holes on top of the Au film which defines the top electrode on the membrane. Second, this pattern is transferred through the gold top electrode, the dielectric layer, and the photoresist layers, and into the bottom gold contact layer. In the third process we use a nickel sulfonate bath to deposit nickel pillars into this anisotropically etched hole. Figures 3(a) and 3(b) show a top view and an angled view of a membrane sample through which an array of holes was etched, followed by nickel plating. The bright spots seen in Fig. 3(a) show the positions of the plated nickel, whereas the dark holes are unplated etched holes. We use the tunneling electrode to plate the tip, and thus only the center electrode is electroplated on. After removal of the

photoresist, the nickel pillars become more easily visible underneath the membrane [Figs. 3(c) and 3(d)]. In the angle micrograph of Fig. 3(d), we can see the nickel tip, and can infer the height of this pillar.

A spiral coil can also be fabricated on top of the deflecting membrane by an additional electron beam lithography and ion milling process, and with a permanent magnet electroplated below this membrane (Fig. 4), can be used to construct an electromagnetic “solenoid”-like deflection system. The membrane deflection can thus also be measured magnetostatically through an induced voltage resulting from the suspended electric coil penetrating through the field lines of the permanent magnet. The geometry of this detection system is analogous to a miniature version of a common microphone. The precise spacing between the membrane and magnet can also be remotely adjusted by using the electrostatic deflector field. This will then allow us to precisely control the sensitivity of this solenoid detector.

III. RESULTS AND DISCUSSION

We have fabricated electrostatically actuated sensors, in which an electrostatic ac field induces motion in the mem-

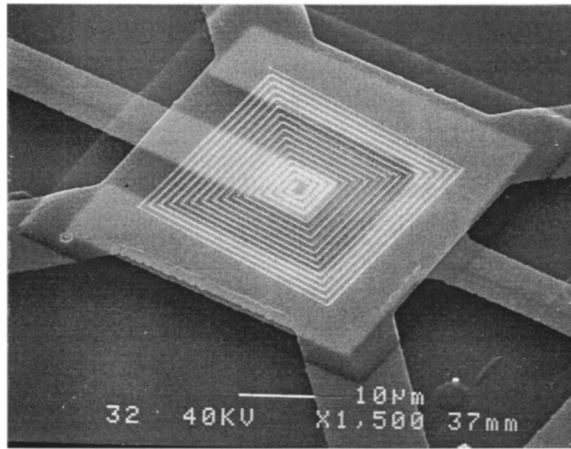
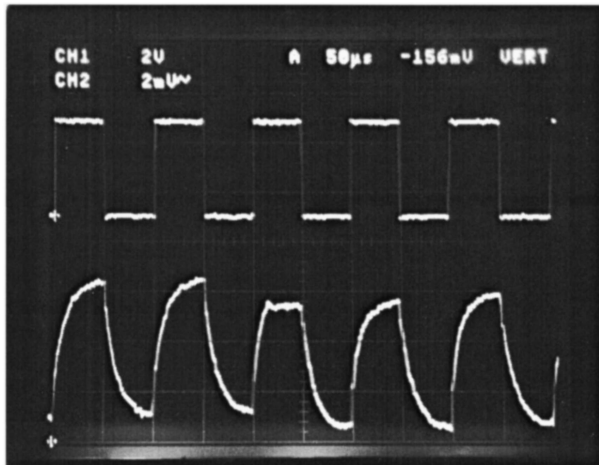
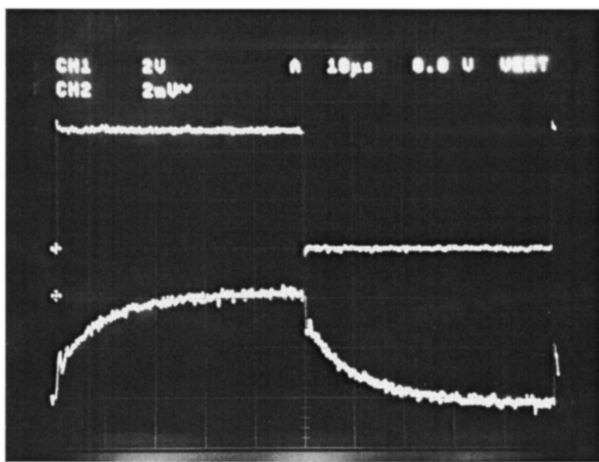


FIG. 4. Close-up view of a sensor device with a patterned gold spiral on the deflection membrane.



(a)



(b)

FIG. 5. (a) Input signal (2.5 V, 10 kHz) and measured response of a vibrating membrane when performing reflectivity measurement of the surface with a 670 nm incident laser beam. (b) Oscilloscope trace showing the response time of the membrane ($\sim 10 \mu\text{s}$) to the electrostatic input signal (2.5 V, 10 kHz).

brane. The amplitude of this motion is then measured independently, while the frequency of the ac field is changed. Maxima in the deflection amplitudes are expected to coincide with resonance conditions for the “vibrating-drum” modes in the membrane. Thus, accurate submicrosecond displacement measurements can be used to monitor and track the plate resonance frequency, which will in turn strongly depend on the absolute mass of the membrane. The frequency of the mn mode transverse vibration of a simply supported square plate with thickness a and length L of the edges is given by:⁴

$$f_{mn} = \frac{\pi a}{2L^2} (m^2 + n^2) \sqrt{\frac{E}{12\rho(1-\sigma^2)}}, \quad (1)$$

where E and σ are the Young's modulus and the Poisson's ratio of the material, respectively. For a 100 nm thick, 50 μm by 50 μm SiO_2 membrane, a fundamental oscillation frequency of about 0.28 MHz is predicted from this equation.

The deflection of the center of such a membrane, during the application of a constant electrostatic field, can also be estimated. The amplitude Δd of a statically deflected metallized membrane separated from a metallized surface (forming a capacitor) by a distance (d) when a voltage (V) is applied can be approximated as:⁴

$$\Delta d = \frac{3\pi V^2 L^4 (\lambda + 2\mu)}{40d^2 \mu (\lambda + \mu) a^3}, \quad (2)$$

where λ and μ are the Lamé constants of the membrane material. From this equation, deflections on the order of 0.1 μm are predicted for applied electrostatic fields of about 5 V.

In the first evaluation experiments, the measurement of the membrane response to electrostatic actuation was undertaken. A laser beam was reflected off a membrane at near-normal incidence in a binocular microscope, and a reverse-biased p - n junction detector was used to detect the reflected light intensity. A function generator was used to generate simple 50% duty cycle actuation signals, and the frequency response of the membrane was measured by observing the detector signal with an oscilloscope. From observation of interference fringes, we find that deflection voltages as low as 1 V already result in $\lambda/4$ ($\sim 100 \text{ nm}$) vertical motion of the membrane, provided that the membrane-substrate distance is small ($< 1.5 \mu\text{m}$). To perform more quantitative frequency response measurements, a HeNe semiconductor laser was used as a directional light source, and deflected off the surface of the membranes, which were electrostatically actuated with a function generator. A silicon detector was used to observe changes of the reflected light intensity, and the measured signal was used to determine the membrane response. The reaction of the membrane to a 2.5 V signal at 10 kHz with 50% duty cycle is summarized in Fig. 5(a). The time-dependent response curve plotted in this oscilloscope trace is limited by the slew rate of the detector, and we observe that the membrane reaction speed exceeds 100 kHz [Fig. 5(b)]. So far, we have not determined the Q of the plate resonance, but expect large dissipation in atmosphere due to the small distance between the vibrating plate and the substrate.

IV. CONCLUSIONS

The fabrication methods developed here are also suitable for the construction of other electrostatically tunable devices and sensors. Therefore, the methodology which will be developed to fabricate chemical detectors can be applied towards a wide variety of surface micromachined detectors, including microfabricated electron tunneling transducers, wavelength-tunable sources and detectors, as well as high spatial resolution magnetometers. Devices which use such tunnel transducers have in the past been constructed by bulk silicon micromachining and include infrared light detectors (Golay cells^{5,6}) and sensitive micromagnetometers. By developing new fabrication techniques which will allow us to generate small electrically controllable deflecting membranes through room-temperature processing, it will be possible to

also integrate these other devices with VLSI driving circuitry and thereby construct many functional monolithic microsensor arrays.

ACKNOWLEDGMENT

This work was funded by the National Science Foundation and the Army Research Office.

¹A. N. Cleland and M. L. Roukes, Appl. Phys. Lett. **69**, 2653 (1996).

²D. W. Carr and H. G. Craighead, J. Vac. Sci. Technol. B, these proceedings.

³L. J. Hornbeck, Appl. Opt. **28**, 4900 (1989).

⁴S. Timoshenko, D. H. Young, and W. Weaver, *Vibration Problems in Engineering* (Wiley, New York, 1974).

⁵T. W. Kenny, J. K. Reynolds, J. A. Podosek, E. C. Vote, L. M. Miller, H. K. Rockstad, and W. J. Kaiser, Rev. Sci. Instrum. **67**, 112 (1996).

⁶T. W. Kenny, W. J. Kaiser, S. B. Waltman, and J. K. Reynolds, Appl. Phys. Lett. **59**, 1820 (1991).